2023 IEEE International Conference on Robotics and Automation (ICRA 2023)
May 29 - June 2, 2023. London, UK

SonicFinger: Pre-touch and Contact Detection Tactile Sensor for Reactive Pregrasping

Siddharth Rupavatharam†, Caleb Escobedo†, Daewon Lee,
Colin Prepscius, Larry Jackel, Richard Howard and Volkan Isler

***Abstract*— Robot end effectors with proximity detection and contact sensing capabilities can reactively position the gripper to align objects and ensure successful grasps. In this paper, we introduce *SonicFinger*, an acoustic aura based sensing system capable of full-surface pre-touch and contact sensing. A single piezoelectric transducer embedded within a novel 3D printed finger is excited using a monotone to create an acoustic aura encompassing the finger; this enables pre-touch sensing and gripper alignment, while changes in finger-transducer acoustic coupling indicate contact. *SonicFinger* is low-cost, compact, and easy to manufacture and assemble. Sensing capabilities are evaluated using a set of objects with various physical properties such as optical reflectivity, dielectric constants, mechanical properties, and acoustic absorption. A dataset with over 8,000 proximity and contact events is collected. Our system shows a pre-touch detection true positive rate (TPR) of 92.4% and a true negative rate (TNR) of 95.3%. Contact detection experiments show a TPR of 93.7% and a TNR of 98.7%. Furthermore, pre-touch detection information from *SonicFinger* is used to adjust the robot grippers pose to align a target object at the center of both fingers.**

I. Introduction

In the past decades, many types of tactile sensors have been developed to improve robot grasping accuracy and reliability. Tactile sensors only provide information post-contact, rendering robots unable to reactively adjust pre-contact to ensure a successful grasp. Several modalities of proximity sensing have been implemented to provide reactive sensing in the pre-touch range (i.e., $\leq$ 10cm) [1]. Despite the existence of many different types of pre-touch and contact sensing modalities on end-effectors [2]–[6], wider adoption of reactive pre-grasping in robotic manipulation remains limited. Sensors that perform (1) pre-touch sensing, (2) object centering, and (3) contact sensing, often do not meet the requirements of being reliable, easy to use, compact, inexpensive, and possessing the ability to sense all around the end-effector without blind spots.

SonicFinger performs pre-touch and contact sensing using a single piezoelectric transducer embedded in a 3D printed finger as shown in fig. 2. Piezos convert electric charge to mechanical vibrations and vice-versa. The piezo embedded in the finger is excited with an alternating voltage to create acoustic vibrations that are transferred to the finger. These vibrations then leak into the air creating an acoustic field or aura as shown in fig. 1. Objects entering this acoustic aura reflect some of the waves back to the finger. The reflected waves are sensed by the transmitting piezoelectric transducer; changes in the reflected waves indicate when objects are in close proximity. When an object touches the finger, changes in the acoustic coupling are easily detected.

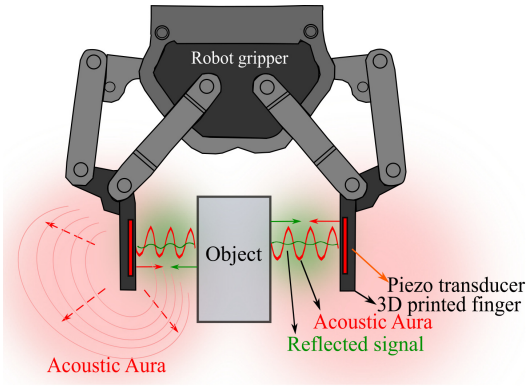

Fig. 1: *SonicFinger* system: a 3D printed finger is attached to a robot gripper with an embedded piezoelectric transducer. The piezoelectric transducer is excited, vibrating itself and the finger. Vibrations from the finger spread into the air nearby, creating an acoustic aura (in red). Objects that enter this aura reflect the aura back to the finger (in green). Changes caused by the reflected signal give pre-touch information.

SonicFinger performs *full-surface* proximity independent of field of view, since acoustic waves are emitted omnidirectionally from the surface. Pre-touch detection of objects with different shapes and sizes, optical, electrical, magnetic, mechanical, and other properties is possible and depends only on object acoustic reflectivity. The pre-touch information from two fingers in a parallel jaw gripper is combined to center objects in between the end effector before grasping. Then, the gripper is closed to bring the fingers into contact with the object. *SonicFinger* informs the robot about the start, persistence, and end of contact.

The contributions of the paper are as follows:

- **Finger design:** A novel low-cost, compact, easy to manufacture and deploy 3D printed finger.
- **Sensing methodology:** A single piezoelectric sensor used to create an aura around the finger and sense changes in reflected signals
- **Signal processing:** A balanced detection circuit and coherent detection pipeline to extract small changes in the reflected signal
- **Algorithms:** New algorithms for pre-touch proximity detection, grasp centering, and contact detection
- **Real-world control:** A real-time system prototyped by attaching two fingers with embedded piezoelectric transducers($<$ \$2) on a Robotiq gripper attached to a

†Authors contributed equally to this work. All authors are with the Samsung AI Center New York, NY.

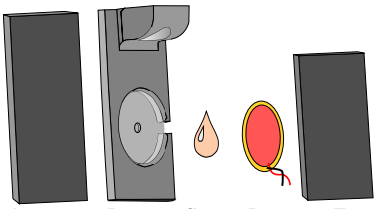

Fig. 2: Exploded view of *SonicFinger*, (A) Foam 1, (B) 3D printed finger, (C) Adhesive, (D) Piezoelectric transducer, (E) Foam 2.

Kinova Gen3 robot arm. Audio acquisition and signal processing tool chains are used to demonstrate *SonicFinger*'s capabilities under several realistic settings.

SonicFinger aims to provide an affordable pre-grasp and contact sensor for reactive pregrasp sensing that is robust and easy-to-use.

II. Related Work

Navarro et. al. [1] define pre-touch range as distances $\leq$ 10cm from the robot surface. Sensing in this range is a precursor to contact based interactions like grasping. Techniques that perform pre-touch and contact sensing are discussed in this section.

1) Capacitive sensing: The electric field around a sensing electrode is measured and changes in it are monitored when objects approach the sensing area. State of the art solutions use multiple electrodes on a single finger to detect object proximity contour, and material detection all around a gripper [3], [4], [7]. Capacitive sensors have also been used to demonstrate reactive preshaping with tactile sensing [8]–[10]. Performance depends on the dielectric constant, coupling to ground, and conductivity properties of objects. It is challenging to sense different objects with the same sensitivity and range. Capacitance is directly proportional to the surface area of the electrode and inversely proportional to the distance between the sensor and the object. To sense all around a finger, multiple sensors of different sizes are needed on an end-effector. Sensor size and placement need to be traded for sensitivity and range. These reasons make it challenging to create a finger that can perform both pre-touch and contact sensing all around an end-effector using only capacitance sensors.

2) Infrared Ranging (IR): These sensors emit electromagentic radiation in infrared wavelengths (700nm - 1mm) and detect reflected radiation. The distance to an object is computed based on the different properties of reflected radiation. Measuring reflected radiation intensity, time of flight, and using multiple sensors to perform triangulation are some techniques used [5], [11]–[17]. Near-field IR sensors are highly directional, requiring a large number of sensors to sense all around the robot. These sensors are able to perform proximity detection but not contact detection and hence require other complementary tactile sensors [18], [19].

3) Acoustic sensing: Traditional ultrasonic sensors use the sonar principle – bursts of reflected audio pulses are used to detect and range objects. Round trip time of an emitted pulse is calculated to obtain object distance and velocity [20]–[24]. Piezoelectric transducers are used to generate ultrasonic (i.e., $\geq$ 40kHz) pulses of sound. Typically two transducers are required, one to transmit and one to receive. The sensors have fixed cones of sensing and multiple sensors are required to cover all sides of a finger. Ultrasonic sensors also have non-negligible offsets and tend to make end-effector fingers bulky. These sensors can detect objects as long as they are acoustically reflective. They can reliably range objects at a distance but do not perform well when objects are very close or in contact with the sensor.

4) Contact sensing: Tactile sensors for in-hand manipulation and contact detection have been proposed. Vision-based tactile sensors measure contact forces as changes in images recorded by a camera, typically through the use of a deformable elastomer. Digit [25], GelSight [26], TacTip [27], are examples among others [6] that belong to this class of sensors. These sensors provide contact, texture, and force information but do not possess any pre-touch sensing capabilities. They also assume implicit contact with objects. The BioTac sensor [28] uses an incompressible liquid as an acoustic conductor to convey vibrations from the skin to a pressure transducer located at the core of a mechatronic finger. The BioTacs sense the smallest vibrations, but the fingers do not provide pre-touch information, are hard to maintain, and require frequent liquid replacement.

5) Acoustic aura sensing: Fan et. al. [29] propose AuraSense, a collision avoidance system that uses an acoustic aura. The surface of a robot is made to vibrate using a mounted piezoelectric transducer. Some of these vibrations leak into the air near the surface of the robot giving rise to an acoustic aura encompassing the robot link. An object brought close to the robot surface sets up a standing wave between itself and the robot surface. This standing waves, along with the interference generated due to the motion of the robot or object, are indicative of a proximity signal. The standing waves and changes in them are sensed using a receiver attached to the robot surface. While it detects proximity, AuraSense does not detect contact. Fan et. al. [30] propose SonicSkin, a contact detection, localization, and pressure estimation system using surface acoustic waves. SonicSkin creates vibrations and detects them on the robot surface in the same manner as AuraSense. Contact is detected by a receiver measuring changes in the signal transmitted on the surface. SonicSkin does not detect objects in close proximity.

SonicFinger uses a single piezoelectric transducer embedded inside a 3D printed finger to create an acoustic aura all around the finger and senses reflections from objects that enter this aura. Compared to other techniques discussed previously, *SonicFinger* performs pre-touch detection, object centering, and contact detection using a single sensor. Objects of different shapes, sizes, dielectric constants, mechanical properties, and electromagnetic reflectivity properties can be detected. *SonicFinger* is compact, easy to deploy, and a low-cost ($\leq$ \$2) solution that works in real-time.

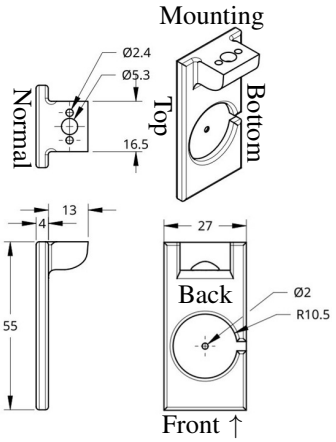

Fig. 3: Orthographic and isometric projections of the 3D printed finger model. Sides of the finger tested during the evaluation section are listed as normal, back, top, bottom, and front.

III. System Design

The system showcases a novel 3D printed finger coupled to a piezoelectric transducer, that performs (i) pre-grasp object detection, (ii) object centering, and (iii) contact detection. Hardware and software methods used to realize the system are discussed in this section.

A. Finger design & construction

We design a finger that is 55mm long, 27mm wide, and 4mm thick with a flat end that easily attaches to different robot end-effectors as shown in fig. 3. The finger has a large sensing and gripping area along with a standard mounting end attached with a single M5 socket headcap screw. It also includes a circular indent 3mm deep where the transducer is embedded. It rests on a thin adhesive layer above a 1mm thick section of the finger. A sprue is made in the center of the indent to allow any excess adhesive to flow out, creating a uniform layer below the transducer. The contact surface and transducer side are covered using 1mm thick foam [31] with backing glue for compliant gripping and transducer protection. Exploded views of the finger and sensor are shown in fig. 2. The side with Foam 1 is used as the contact surface (i.e., normal). The foam was chosen as it couples acoustically well to transfer vibrations from the finger to the air while being supple and flexible, while allowing the finger to be placed in several positions and exert different forces on an object.

This finger design is able to grab, pick, lift and place objects while protecting the piezoelectric transducer embedded within from physical damage. It is compact in size, quick to deploy, low in cost, and easy to manufacture in large numbers. From a sensing standpoint, the finger material and design couple acoustically with the piezoelectric transducer to vibrate and produce an acoustic aura.

1) Piezoelectric transducers and acoustic coupling: Piezoelectric materials vibrate in response to applied electric charge and generate an electric charge in response to applied mechanical stress [32]. *SonicFinger* uses an ultrasonic AC signal to excite a Lead Zirconate Titanate (PZT) piezoelectric crystal transducer to vibrate a robot finger and create an acoustic aura engulfing it. Objects in close proximity that enter the acoustic aura reflect audio signals back to the finger and get sensed by the same piezoelectric transducer that created the acoustic aura.

Vibrations originating from the transducer are transferred from the (i) transducer to the finger, (ii) finger to the foam, and (iii) foam to air. This transfer of energy from one layer to the next depends on the acoustic matching at each transition junction and are influenced by finger thickness and material properties. With acoustically matched transitions transmitting and receiving vibrations with fewer losses overall. While our system was realized using empirical matching, a bespoke acoustic transmission stack would improve performance. As discussion of such a design is beyond the scope of this paper, we leave it for future work.

2) Excitation frequency: An ultrasonic excitation frequency is selected as it is inaudible and its wavelength is appropriate for the size scale of the fingers. A linear chirp signal [33] is used to excite the piezoelectric transducer embedded in the finger to determine a frequency that transfers best across multiple layers of the finger. For our stack, 40kHz at $18V_{rms}$ is the optimal frequency for sensing both proximity and contact.

B. Circuit and signal processing pipeline

Acoustic signals reflecting off of objects that enter the aura as illustrated in fig. 1 need to be detected to obtain object pre-touch and contact information. A balancing circuit such as the Wheatstone bridge, is used to detect these low amplitude reflected signals occurring in the backdrop of the larger transmit signal. A Wheatstones bridge is a null measurement technique circuit containing two voltage dividers forming two arms of a bridge that are excited using a common source voltage. With the voltage difference across the two arms, $(A - B)$, considered as the output voltage. When the voltage across both the arms is the same, the bridge is said to be balanced producing $(A - B) = 0$ V. Even a small voltage change in either arm results in the bridge going out of balance, and is indicated by $A - B \neq 0$ V. Conventionally, a measurement is made with the voltage of one arm varying with respect to a static reference voltage on the other. *SonicFinger* uses a resistor in series with a transducer embedded inside a finger for one arm of the bridge (i.e., variable), and a resistor in series with a matched impedance similar to the transducer embedded inside a finger for the other (i.e., reference). Output from each of the arms A and B are fed to the inverting and non-inverting terminals of a differential amplifier to perform subtraction. Objects that enter the acoustic aura reflect acoustic waves back to the finger disturbing the balance of the bridge, producing a voltage change. Additionally, the high amplitude transmitted signal common to both arms gets subtracted leaving behind the low amplitude reflected signal. Output of the differential amplifier is at the transmitted frequency with the pre-touch information appearing as undulations in the envelope of the signal as shown in fig. 4a.

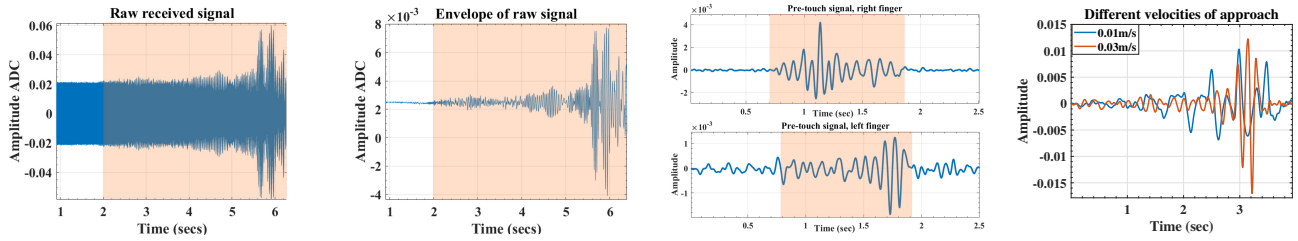

(a) (b) (c) (d)

Fig. 4: (a) Raw received signal at 40kHz (dark blue signal) with pre-touch information present in the envelope (red region), (b) Extracted envelope from raw received signal using signal processing pipeline, (c) Pre-touch signals (in red) from right finger (top) and left finger (bottom) deployed on a parallel jaw gripper, and (d) A finger approaches a 1.905cm PVC pipe with two different velocities, 0.01m/s and 0.03m/s. Faster velocity produces same number of oscillations as slower velocity, but more closely spaced and larger amplitude.

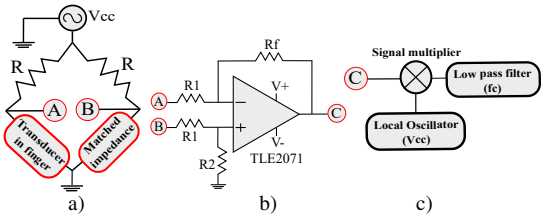

Fig. 5: Signal processing blocks: a) Wheatstones bridge circuit, b) Differential amplifier circuit, c) Signal mixing pipeline.

The next step is to extract the information present in the envelope, which is performed using signal mixing followed by low pass filtering. A signal mixer is used to multiply the output of the differential amplifier with an in-phase copy of the transmitted signal. The multiplication results in a DC level change proportional to the undulations on the envelope and a high frequency term that is easily filtered out using a low pass filter with an appropriate cut off frequency. The reflected signal information present in the undulations is obtained. The complete signal processing schema is shown in fig. 5, with $R = 2.2\text{k}\Omega$, $R_1 = 3\text{k}\Omega$, and $R_2 = R_f = 100\text{k}\Omega$.

C. Pre-touch detection

An end-effector equipped with two fingers is moved towards an object, making it enter the aura. Acoustic waves reflecting off the object are sensed by the transducers embedded in each finger, with the reflected signal strength depending on the distance from each finger. The reflected signals interfere with transmitted signals and appear as undulations in the envelope of the signal output by the transducer as shown in fig. 4b. These undulations are independent of the robot speed and represent nodes at a specific distance as the robot approaches the object. At a different speed we will see the same amount of undulations. The method used to extract proximity information from the undulations are described next.

The amount of signal reflected back to the sensor is a function of the objects position, velocity, shape, mechanical properties, and size. As the object moves closer to the finger, greater amounts of transmitted signals are reflected back, increasing the amplitude of the interference or undulations. The velocity of the object affects the rate at which the signal oscillates. The signal oscillates as the distance between the object and the finger changes. Faster moving objects create closely spaced undulations, while slower objects create the same number, but more spread out as shown in fig. 4d. Therefore, proximity is detected by monitoring the amplitude and quantity of undulations. While robot motion and non-proximity signals appear as noise with their spectral power spread out over various frequencies, undulations have frequencies below 100 Hz when proximity is present. Hence, a threshold based on summed spectral power is proposed to identify the characteristic proximity pattern in real-time.

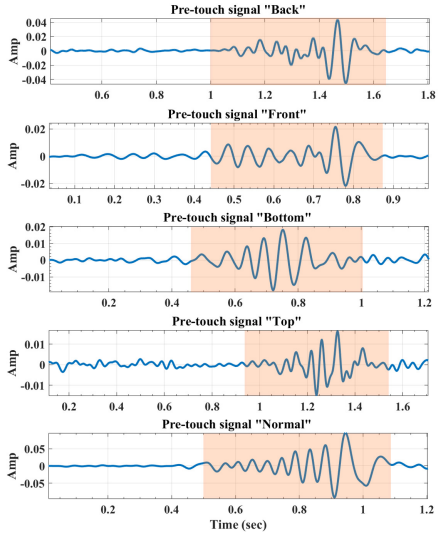

Fig. 6: Full surface pre-touch signals for each side of the finger. The red shaded region shows proximity signals when approaching a 1.905cm PVC pipe.

The undulation signal, $y(t)$ is divided in to windows α seconds long, and a Fourier Transform is used to obtain the spectral information $Y_\alpha(\Omega)$ present in each time window $y_\alpha(t)$. The Fourier Transform is given by,

$$Y(\Omega) = \int_{-\infty}^{\infty} y(t) e^{-i2\pi\Omega t} dt, \quad \forall \Omega \in \mathbb{R}. \tag{1}$$

The Fourier Transform decomposes a time domain signal into its constituent frequency components and provides magnitude of each frequency present in the waveform. As noted previously, frequencies less than 100 Hz have higher magnitudes compared to other frequencies when a proximity pattern exists. The spectral powers between $0 - 100$Hz are summed and compared to a heuristic threshold, γ. If the summed spectral power is greater than the threshold, a proximity event is detected.

D. Object centering

Two fingers are deployed on a parallel jaw robot gripper and proximity signals from each finger are compared to estimate the position of an object present in between the fingers. A stronger proximity signal is sensed from the finger closest to the object. To perform object centering, the robot moves along a single axis perpendicular to an object. When the object is detected by either finger the end-effector position is saved and velocity changed to move the opposite finger towards the object. The second finger then detects the object. The average of the two detection locations is computed and the robot gripper moved to the middle of both positions, centering the object using only pre-touch information. The proximity signals from both fingers for an object in between them are shown in fig. 4c.

E. Contact detection

Prior to contact, the characteristic proximity pattern is observed as the finger approaches an object. This is followed by a sharp level change as soon as the finger makes contact and remains constant for as long as the contact is maintained using the same force. Once the contact ends, there is another level change returning the signal back to the previous no-contact level, followed by a proximity pattern corresponding to the finger moving away. Additionally, a short rise and fall time just before the signal stabilizes to a level change is observed. This is attributed to the time it takes the gripper to reach a constant applied force. Signal changes corresponding to contact are explained by modeling the combination of a vibrating transducer and the finger it is embedded in as having a certain acoustic coupling. Voltage changes across the piezoelectric transducer occur as the combined acoustic coupling changes when the finger makes contact with an object. An illustration of how the signal changes when different sides of the finger make contact with an object are shown in fig. 7.

A z-score algorithm is used to perform contact detection, as the signal level changes due to contact are large, distinct, and constant compared to no contact. Z-score is a statistical measure that informs how far away a data point is from the rest of the data and how many standard deviations away a given observation is from the mean.

$$z_{score}(n) = \frac{y(n) - mean(y)}{std(y)} \tag{2}$$

$$\text{Contact} = \begin{cases} 1, & \text{abs}(z_{score}(n)) > \gamma \\ 0, & \text{otherwise.} \end{cases} \tag{3}$$

Where, y(n) is the next incoming processed sample and γ is a heuristically set threshold.

IV. Evaluation and Results

The evaluation of our system is split into two categories: Sensor characterisation and real-world deployment. Sensor characterisation is performed using a single PVC pipe 1.905cm in diameter and 25.4cm in length. Real-world deployment evaluation uses objects with a variety of sizes, shapes, and material properties. The objects have different optical reflectivity, dielectric constants, and acoustic absorption properties and are shown in fig. 8a. Full surface pre-touch and contact detection are evaluated along with object centering.

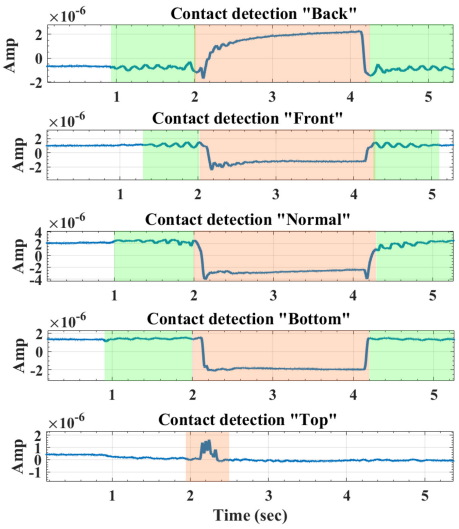

Fig. 7: Full surface contact signals for each side of the finger. The green shaded region show proximity signals when approaching and moving away from the object. The peach shaded region is the duration of contact with the object.

SonicFinger is deployed on a Kinova Gen3 robot arm equipped with a Robotiq 2F-85 gripper for all experiments [34]. A cartesian-velocity controller is used to specify speed and direction of the robot end-effector. Two 3D printed fingers are integrated in the parallel jaw gripper as shown in fig. 8b. Each finger has a single piezoelectric transducer (CPT-2065-L100) [32] embedded in it and is attached to the gripper using a single M5 socket headcap screw. Fingers are constructed using Formlabs Grey Pro resin and a Form 3+ 3D printer. A Zoom F8N Field Recorder with USB Audio Interface is used as the analog to digital converter (ADC) to digitize and acquire the signal. The sampling rate for the ADC is 96 kHz with a bit depth of 24 bits. Signal processing is performed on an Intel NUC7i7BNH computer.

A. Sensor characterisation

1) Full surface pre-touch detection: SonicFinger is evaluated on its ability to detect proximity to a 1.905cm PVC pipe placed at a known fixed location. The robot gripper is moved towards the stationary pipe in three different axes. The axes are shown in fig. 8b. Along the x-axis, the gripper is moved perpendicular to the object from a distance of 5.5cm to 0.4cm from the object; y-axis, from 4cm till the object is within the parallel jaw gripper; z-axis, up and down lengthwise along the side of the pipe at a distance of 3cm. This is to characterize the pre-touch sensing of the "normal" side of the finger. Next, pre-touch sensing of the other four sides of the finger (i.e., back, front, top, bottom) are characterized. The end-effector is rotated to align each side along the x-axis and approach from a distance of 5.5cm to 0.4cm from the PVC pipe. Processed signal output from each side is shown

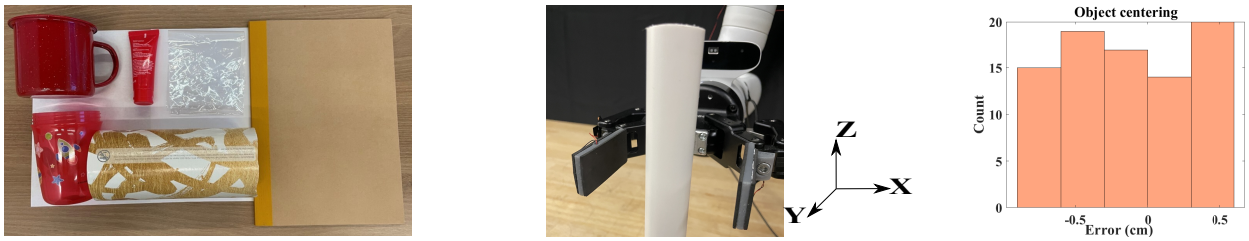

(a) (b) (c)

Fig. 8: (a) All objects used in the real-world evaluation of SonicFinger. Objects top left to right: mug, hand sanitizer, transparent plastic, notebook, water cup, and paper cylinder, (b) Robot gripper equipped with two *SonicFinger*'s performing grasp centering on a 1.905cm PVC pipe, and (c) Histogram of object centering results, maximum error of 0.8cm.

in fig. 6. These signals are then processed using the pre-touch detection algorithm presented in section III-C. All sides are able to perform pre-touch detection.

2) Object centering: A pair of fingers are evaluated on their ability to center an object with no contact as shown in fig. 8b. In this scenario, the PVC pipe is positioned in one of three locations inside the gripper; (i) close to the right finger, (ii) close to the left finger, and (iii) near the center. The robot centers based on the algorithm presented in section III-D. 85 trials of centering are conducted and the results are shown in fig. 8c. The histogram shows a slight skew towards the negative error side. The two fingers used for our evaluations are not identical in their construction which leads to the slight offset in centering that is observed.

3) Full surface contact detection: SonicFinger is evaluated on its ability to detect contact with a 1.905cm PVC pipe placed at a known fixed location. The robot gripper is moved from a predefined position to a position in physical contact with the pipe. Each of the five sides of the finger are made to contact the pipe. As shown in fig. 7 a level shift occurs when the finger makes contact with the PVC pipe. This is seen around the 2s mark for each side of the finger. The level shift persists as long as the finger remains in contact with the pipe as seen from the 4s mark. The contact detection algorithm discussed in section III-E is used to process these signals. Contact is detected 100% from all sides of the finger except for the top.

B. Real-world deployment

Objects shown in fig. 8a are used to evaluate sensor performance in a real-world settings. Over 8,000 pre-touch, contact and object centering data points are collected using these objects. These objects are curated for their varying optical reflectivity, dielectric constants, and acoustic absorption properties. The ground truth centering locations are manually measured in the robot base frame and compared against the purposed center location for each object; the final end-effector location for each centering trial. Both of the robot gripper fingers are active simultaneously during the deployment. Minimal interference was observed even with the sensors operating at the same frequency.

1) Full surface pre-touch: The fingers are used to approach each of the objects from the real-world object set. A pre-touch sensing true positive rate (TPR) of 92.4% and a true negative rate (TNR) of 95.3% is obtained. The system is able to detect objects that are transparent, similar in dielectric constants and conductivity, different shapes and sizes. Soft objects absorb sound making them relatively harder to detect.

2) Object centering: The fingers are used to center the objects from the real-world object set. *SonicFinger* shows object centering performance similar to the sensor characterization tests.

3) Full surface contact: The fingers are used to make contact each of the objects from the real-world object set. *SonicFinger* shows a contact sensing TPR 93.7% and a TNR of 98.7%.

V. Conclusion and Discussion

Sensing systems that can perform both pre-touch and contact detection enable reactive preshaping and contact confirmation. State of the art robot grippers use multiple modalities to perform pre-touch and contact sensing simultaneously. In this work, we present *SonicFinger*, an acoustic aura based sensing system capable of pre-touch sensing, object centering, and contact detection using a single piezoelectric transducer embedded within a 3D printed finger. The piezoelectric transducer vibrates the finger to create an acoustic aura that encompasses the full surface of the finger. Objects that enter this aura reflect signals back to the finger and indicate proximity, while objects that make contact with the finger, change its acoustic coupling. The system is evaluated on a set of objects with physical properties such as acoustic absorption, optical reflectivity and dielectric constants. Based on our sensor characterization and real-world experiments, *SonicFinger* can be used as a low cost, compact, easy to deploy pre-touch and contact sensor for robot manipulators.

Future work can extend *SonicFinger* to investigate pre-touch and contact sensing with an object in-hand to help placing objects in a cluttered scenes. Additionally, a temporal difference may be used to determine which surface on the finger an object is being sensed in relation to. For example, if a robot is moving downwards and detects an object is close proximity, it is most likely that this object is below the gripper based on the direction of movement. Force information could possibly be gathered from the contact signal based on previous work analyzing a frequency chirp sent over a robot arm [30].

References

[1] S. E. Navarro, S. Mühlbacher-Karrer, H. Alagi, H. Zangl, K. Koyama, B. Hein, C. Duriez, and J. R. Smith, "Proximity perception in human-

centered robotics: A survey on sensing systems and applications," *IEEE Transactions on Robotics*, 2021.

[2] L.-T. Jiang and J. R. Smith, "Seashell effect pretouch sensing for robotic grasping." in *ICRA*. Citeseer, 2012, pp. 2851–2858.

[3] J. R. Smith, E. Garcia, R. Wistort, and G. Krishnamoorthy, "Electric field imaging pretouch for robotic graspers," in *2007 IEEE/RSJ International Conference on Intelligent Robots and Systems*. IEEE, 2007, pp. 676–683.

[4] R. Wistort and J. R. Smith, "Electric field servoing for robotic manipulation," in *2008 IEEE/RSJ International Conference on Intelligent Robots and Systems*. IEEE, 2008, pp. 494–499.

[5] R. Patel, R. Cox, and N. Correll, "Integrated proximity, contact and force sensing using elastomer-embedded commodity proximity sensors," *Autonomous Robots*, vol. 42, no. 7, pp. 1443–1458, 2018.

[6] K. Shimonomura, "Tactile image sensors employing camera: A review," *Sensors*, vol. 19, no. 18, p. 3933, 2019.

[7] B. Mayton, L. LeGrand, and J. R. Smith, "An electric field pretouch system for grasping and co-manipulation," in *2010 IEEE International Conference on Robotics and Automation*. IEEE, 2010, pp. 831–838.

[8] S. E. Navarro, M. Schonert, B. Hein, and H. Wörn, "6d proximity servoing for preshaping and haptic exploration using capacitive tactile proximity sensors," in *2014 IEEE/RSJ International Conference on Intelligent Robots and Systems*. IEEE, 2014, pp. 7–14.

[9] S. E. Navarro, F. Heger, F. Putze, T. Beyl, T. Schultz, and B. Hein, "Telemanipulation with force-based display of proximity fields," in *2015 IEEE/RSJ International Conference on Intelligent Robots and Systems (IROS)*. IEEE, 2015, pp. 4568–4574.

[10] D. Goeger, M. Blankertz, and H. Woern, "A tactile proximity sensor," in *SENSORS, 2010 IEEE*. IEEE, 2010, pp. 589–594.

[11] K. Hsiao, P. Nangeroni, M. Huber, A. Saxena, and A. Y. Ng, "Reactive grasping using optical proximity sensors," in *2009 IEEE International Conference on Robotics and Automation*. IEEE, 2009, pp. 2098–2105.

[12] D. G. Wegerif and D. J. Rosinski, "Sensor-based whole-arm obstacle avoidance for kinematically redundant robots," in *Sensor fusion V*, vol. 1828. SPIE, 1992, pp. 417–426.

[13] G. Petryk and M. Buehler, "Dynamic object localization via a proximity sensor network," in *1996 IEEE/SICE/RSJ International Conference on Multisensor Fusion and Integration for Intelligent Systems (Cat. No. 96TH8242)*. IEEE, 1996, pp. 337–341.

[14] P. Mittendorfer and G. Cheng, "Humanoid multimodal tactile-sensing modules," *IEEE Transactions on robotics*, vol. 27, no. 3, pp. 401–410, 2011.

[15] B. Yang, P. Lancaster, and J. R. Smith, "Pre-touch sensing for sequential manipulation," in *2017 IEEE International Conference on Robotics and Automation (ICRA)*. IEEE, 2017, pp. 5088–5095.

[16] K. Huang, P. Lancaster, J. R. Smith, and H. J. Chizeck, "Visionless tele-exploration of 3d moving objects," in *2018 IEEE International Conference on Robotics and Biomimetics (ROBIO)*. IEEE, 2018, pp. 2238–2244.

[17] C. Escobedo, M. Strong, M. West, A. Aramburu, and A. Roncone, "Contact anticipation for physical human–robot interaction with robotic manipulators using onboard proximity sensors," in *IEEE IROS 2021*.

[18] R. Patel and N. Correll, "Integrated force and distance sensing using elastomer-embedded commodity proximity sensors." in *Robotics: Science and systems*, 2016.

[19] R. Patel, J. C. Alastuey, and N. Correll, "Improving grasp performance using in-hand proximity and dynamic tactile sensing," in *International Symposium on Experimental Robotics*. Springer, 2016, pp. 185–194.

[20] M. Toa and A. Whitehead, "Ultrasonic sensing basics," *Dallas: Texas Instruments*, 2020.

[21] Z. Tong, H. Hu, Z. Wu, S. Xie, G. Chen, S. Zhang, L. Lou, and H. Liu, "An ultrasonic proximity sensing skin for robot safety control by using piezoelectric micromachined ultrasonic transducers (pmuts)," *IEEE Sensors Journal*, 2021.

[22] I.-J. Cho, H.-K. Lee, S.-I. Chang, and E. Yoon, "Compliant ultrasound proximity sensor for the safe operation of human friendly robots integrated with tactile sensing capability," *Journal of Electrical Engineering and Technology*, vol. 12, no. 1, pp. 310–316, 2017.

[23] U. Nunes, P. Faia, and A. T. de Almeida, "Sensor-based 3-d autonomous contour-following control," in *Proceedings of IEEE/RSJ International Conference on Intelligent Robots and Systems (IROS'94)*, vol. 1. IEEE, 1994, pp. 172–179.

[24] P. Dario, A. Sabatini, B. Allotta, M. Bergamasco, and G. Buttazzo, "A fingertip sensor with proximity, tactile and force sensing capabilities," in *EEE International Workshop on Intelligent Robots and Systems, Towards a New Frontier of Applications*. IEEE, 1990, pp. 883–889.

[25] M. Lambeta, P.-W. Chou, S. Tian, B. Yang, B. Maloon, V. R. Most, D. Stroud, R. Santos, A. Byagowi, G. Kammerer *et al.*, "Digit: A novel design for a low-cost compact high-resolution tactile sensor with application to in-hand manipulation," *IEEE Robotics and Automation Letters*, vol. 5, no. 3, pp. 3838–3845, 2020.

[26] W. Yuan, S. Dong, and E. H. Adelson, "Gelsight: High-resolution robot tactile sensors for estimating geometry and force," *Sensors*, vol. 17, no. 12, p. 2762, 2017.

[27] B. Ward-Cherrier, N. Pestell, L. Cramphorn, B. Winstone, M. E. Giannaccini, J. Rossiter, and N. F. Lepora, "The tactip family: Soft optical tactile sensors with 3d-printed biomimetic morphologies," *Soft robotics*, vol. 5, no. 2, pp. 216–227, 2018.

[28] J. A. Fishel and G. E. Loeb, "Sensing tactile microvibrations with the biotac—comparison with human sensitivity," in *2012 4th IEEE RAS & EMBS international conference on biomedical robotics and biomechatronics (BioRob)*. IEEE, 2012, pp. 1122–1127.

[29] X. Fan, R. Simmons-Edler, D. Lee, L. Jackel, R. Howard, and D. Lee, "Aurasense: Robot collision avoidance by full surface proximity detection," in *2021 IEEE/RSJ International Conference on Intelligent Robots and Systems (IROS)*. IEEE, 2021, pp. 1763–1770.

[30] X. Fan, D. Lee, L. Jackel, R. Howard, D. Lee, and V. Isler, "Enabling low-cost full surface tactile skin for human robot interaction," *IEEE Robotics and Automation Letters*, vol. 7, no. 2, pp. 1800–1807, 2022.

[31] "Michael's creatology foam," 2022, [Online; accessed Sept-016-2022]. [Online]. Available: $https://www.michaels.com/9x12-bright-foam-sheets-by-creatology-40ct/10662178.html$

[32] "Piezoelectric transducer - cui devices cpt-2065-l100," $https://www.mouser.com/datasheet/2/670/cpt_2065_l100-1777538.pdf$, 2022, [Online; accessed Sept-07-2022].

[33] "Linear chirp," 2022, [Online; accessed Sept-016-2022]. [Online]. Available: $https://en.wikipedia.org/wiki/Chirp$

[34] "Robotiq fingertip bundle," $https://blog.robotiq.com/hubfs/Fingertips_bundle_EN_2021-09.pdf$, 2022, [Online; accessed Sept-04-2022].